

# **Improving Tensile Mechanical Properties of FDM-Manufactured Specimens via Modifying Build Parameters**

Mohammad Shojib Hossain, Jorge Ramos, David Espalin, Mireya Perez, Ryan Wicker  
W.M. Keck Center for 3D Innovation, Department of Mechanical Engineering, The University  
of Texas at El Paso, 500 W University Ave, El Paso, TX79968

Accepted August 16th 2013

## **Abstract**

In this paper, the focus was on improving tensile mechanical properties of FDM-manufactured parts by adjusting FDM processing parameters and analyzing stress concentration features between adjacent roads of material. FDM processing parameters are specified by the user via Insight – the file preparation software for most FDM machines. Even though Insight gives the impression that adjacent roads are to be deposited and connected throughout, an optical imaging observation of the deposited material revealed that adjacent roads are not consistently connected forming voids that reduce mechanical performance. Therefore, this work reports the tensile mechanical properties of specimens built using three sets of parameters: standard/default parameters, an Insight revision method, and a visual feedback method. When compared to the default build parameters, the experimentally determined, visual feedback approach produced specimens, in some cases, exhibiting as high as 19% improvement in ultimate tensile strength.

## **Introduction**

The material extrusion additive manufacturing (AM) process [1], commonly known as fused deposition modeling (FDM) is well known for its use in producing prototypes for concept modeling, pre-surgical models in medical applications, and various other uses. Now, efforts have been focused on transforming the technology towards manufacturing production-grade and end-use products [2]. With the current expansion of different material extrusion AM machines, such as the FDM series including the Fortus models and uPrint (Stratasys Inc., Eden Prairie, MN), Makerbot Replicator™ (Makerbot™, Brooklyn, NY ), and numerous other desktop machines, there are various options for processing parameters such as build orientation, raster angle, contour width, raster width, raster to raster air gap, and more. Some software packages have limited access to the processing parameters, by only providing access to build styles (e.g., sparse, solid), hindering the effort to perform process optimization due to the lack of access to raster widths and contour widths, for example. Along with other manufacturing processes, FDM process parameters play a significant role in the performance of the fabricated parts, especially in regards to mechanical properties. For a better understanding of these parameters, a brief description of the FDM operation is provided here.

The main principle of FDM technology is to generate parts directly from three dimensional computer aided design (CAD) data by using a material extrusion process. In most cases, final parts do not require machining. First, a three dimensional CAD model is created and sent to the specific AM software package. The software package used for FDM and Fortus machines is Insight (Stratasys Inc., Eden Prairie, MN). The model is sliced layer by layer within

the Insight job file. Then, toolpaths are generated based on user-specified parameters, which are described here. A rendering of the toolpaths is given by the software. After tooling information, created by Insight, is sent to the FDM machine, a thermoplastic filament is driven into the heated liquefier (Fig. 1) where the plastic reaches a flowable state, and is extruded through a small diameter tip. During deposition of material, the tip moves in the X and Y directions, to create a layer consisting of contour and rasters. Contour creates the peripheral shape of the 3D model and raster is the internal fill pattern in-between the contours. Normally, to hold the whole part in place on the platform, and for building overhanging features, a sacrificial support material is used, which can be broken away or dissolved in a cleaning solution, once the part is completely built. After creating one layer, the bed drops down a distance equal to the height of the layer and a new layer is then deposited over the previous one. This process of building layers subsequently goes on, until the whole part is complete. To maintain a constant heated environment, the entire process is done in a closed chamber which is also known as the envelope. This heated environment helps to improve the interlayer bonding [3] and reduces shrinking, warping and internal stresses [4].

The FDM processing parameters include build orientation, raster angle (RA), contour width (CW), number of contours, raster width (RW), raster to contour air gap, raster to raster air gap (RRAG) and slice height. In this paper, RA, CW, RW, and RRAG were varied using one specific build orientation. The build orientation is the orientation of the part with respect to build platform. According to the ASTM F2921-11 standard, the coordinate system of the build platform and the specific build orientation, in this case XYZ, are shown in Fig. 2. RA is the angle created by the raster and the positive X direction of the build platform. CW and RW is the width of contour and raster, respectively. RRAG is the distance between the edges of two adjacent rasters (Fig.3). A negative RRAG (obtained by decreasing RRAG from zero) causes the partial overlap between two adjacent rasters.

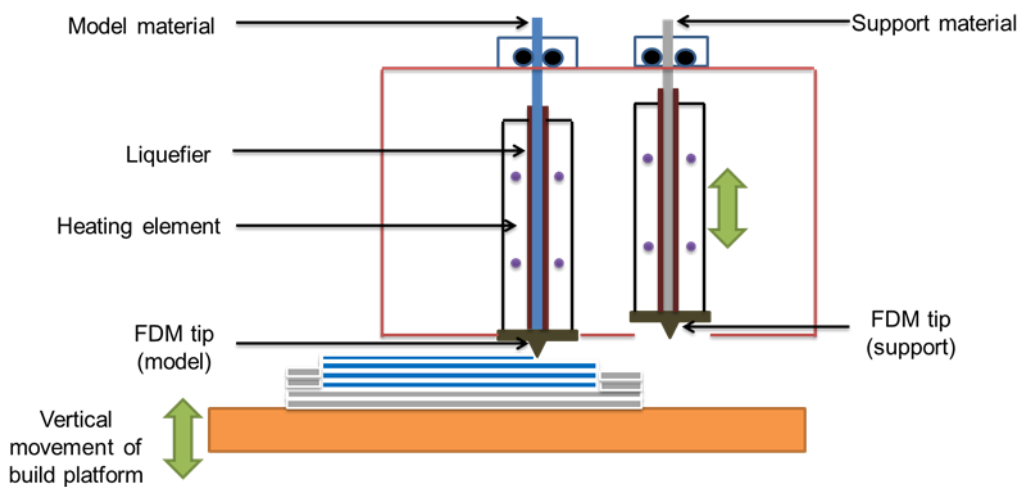


**Fig. 1** Schematic diagram of FDM machine

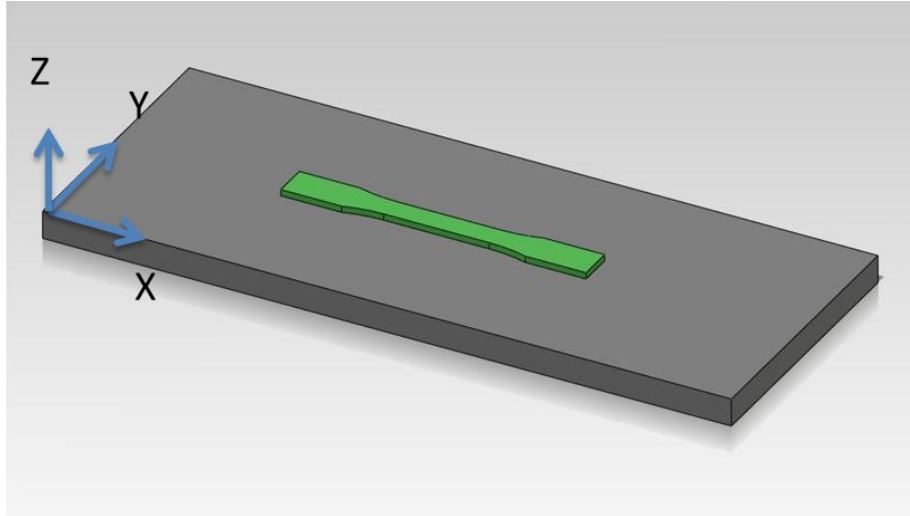


**Fig. 2** XYZ build orientation used for the fabrication of ASTM D638 Type I specimens. The XYZ terminology is based on ASTM F2921-11

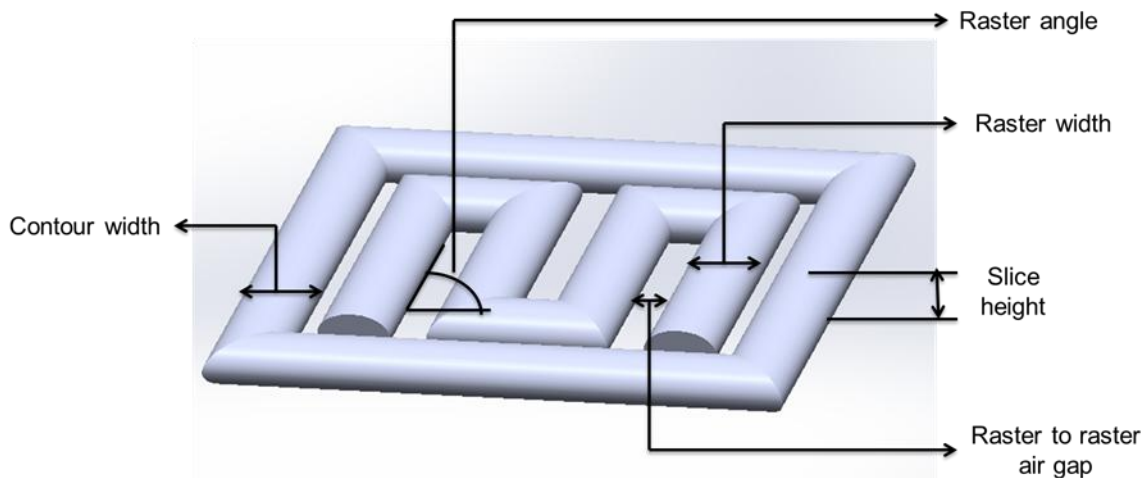


**Fig. 3** FDM Build Parameters

The choices of commercially available thermoplastic materials, for the use with FDM includes acrylonitrile butadiene styrene (ABS), polycarbonate (PC), a PC-ABS blend, polyphenylsulfone (PPSF), ULTEM, and several varieties of the aforementioned materials designed for biocompatible or static dissipation applications [5]. Prior literature also mentioned, other materials processed by FDM including polycaprolactone (PCL) [6], polymethyl methacrylate (PMMA) [7], and composites that contain ceramic, glass, or metal fillers [8, 9]. In this experiment, PC was chosen because of its common use with FDM. Benefits of the material include its high ultimate tensile strength (UTS) (approximately twice of ABS), high hardness, and high toughness. Prior works showed similar testing mostly with ABS, however a data set for PC can be of great use to the FDM community.

Prior efforts have been made towards the modification of FDM-build parameters for improvement in mechanical properties. A Study by Masood *et al.* showed that the UTS of PC decreased about 8% and 13% using two different RWs of 0.4064 mm and 0.6064 mm respectively, while changing the RA from 45°/-45° to 90°/0° [10]. In the same study, the increase of UTS was around 18% by changing the RA from 45°/-45° to 90°/0° using a RW of 0.8314 mm. The highest UTS obtained in that experiment was 58.8 MPa using a RA of 45°/-45° and a RW of 0.6064 mm. Ahn *et al.* tested the same idea of changing the RA, using ABS as the build material and found an increase of about 8%, by changing the RA from 45°/-45° to 90°/0° using RWs of 0.508 mm and 1 mm [11]. In their tests, there was less than a 2% change in UTS using different RWs. In addition, they detected increased build times using small RWs. On the other hand, using ABS, Sood *et al.* observed that, a change in RA from 60°/-30° to 90°/0° led to a decrease in UTS by approximately 19% [12]. The author stated, this was because a 0° RA yielded the longest rasters which led to an increase in stress accumulation along the deposition direction of ABS, resulting in higher distortion and weak bonding. Regarding RRAG on UTS, Ahn *et al.* revealed that a RRAG of -76.2 μm (-0.003 in) increased the tensile strength of ABS by around 30% using a RA of 0°/90° in comparison to a RRAG of 0 mm [11]. Negative air gaps developed dense structures which led to greater UTS. On the contrary, the study by Sood *et al.* revealed that a positive RRAG caused the material to flow between adjacent layers, increasing the bonding between surfaces [12], which led to an increase of around 15% when building with thinner layers, such as 0.127 mm. Changing layer thickness to 0.254 mm, showed no significant difference in UTS using different RRAGs. However, it was unclear if the flow between layers was the result of other factors, such as heat dissipation.

As stated above, a survey of the literature revealed prior work that has been done to improve the mechanical properties through the modification of build parameters. The work presented here emphasizes on establishing a method, which includes optical feedback, to expose the reason for improvement in mechanical properties of PC specimens: UTS, Young's modulus, and tensile strain. Throughout the experiment, it was revealed that the removal of air gaps between adjacent rasters and between contours and rasters, appeared to have a positive effect on mechanical properties. Two methods for modifying the build parameters were developed by considering the toolpath renderings and by examining low-magnified optical images of the test specimens. These methods were compared with default build parameters. It was revealed that the UTS could be improved as high as 19% compared to specimens built using default parameters. Overall, a maximum UTS of 53.75 MPa was attained, as compared to 46.84 MPa using default parameters.

## **Experimental Process**

### **Parameter Modifications**

The test specimen was created according to the ASTM D638 Type I specimen [13] using SolidWorks (Dassault Systemes SolidWorks Corp, Velizy, France). The XYZ build orientation was selected for all the test specimens. For this orientation, three different RAs were used: 0°/90°, 30°/-60°, and 45°/-45°. Three methods were tested to establish the build parameters:

- Default method
- Insight revision method
- Visual feedback method

For the default method, the building parameters were obtained from the default value provided by Insight. Gaps shown in optical images revealed the need for parameter modification. For the Insight revision method, the job files created via Insight software were analyzed. The CW and RW were changed from 0.4064 mm to 0.8128 mm in increments of 0.0254 mm using a 0°/90° RA. From all the combinations of CW and RW, the rendered image showing the smallest gaps between adjacent rasters and contour was selected for building. After that, those parameters were applied to the other two RAs (30°/-60° and 45°/-45°). The gaps between rasters and contour were much more apparent in the rendering for a 0°/90° RA. Therefore, this particular RA was chosen as a modification basis. The parameters that showed better renderings for the 0°/90° RA had a tendency to yield good results for the other RAs. For the visual feedback method, the specimens built with the Insight revision method were analyzed with a microscope. Gaps were visible between two adjacent rasters, though these were not identifiable in the rendering created by Insight. Five different RRAGs, from -0.0025 mm to -0.0254 mm, were analyzed with the microscope. As optical images for a -0.013 mm RRAG displayed an absence of air gaps between two adjacent rasters, it was selected as the best value. The building values are shown in Table 1.

Specimen Construction:

The specimens were built with a Fortus 900 mc (Stratasys Inc., Eden Prairie, MN). According to the manufacturer’s specifications, this machine has a build chamber of 914 mm × 610 mm × 914 mm. PC support was used as support material. The model material, support material, and envelope temperatures were 345°C, 365°C, and 140°C respectively (these are standard model, support, and envelope temperatures for the PC and PC Support materials provided by Stratasys). The layer thickness or slice height was set at 0.254 mm.

Optical evaluation:

A Retiga 2000R fast charge-coupled device camera (QImaging, Surrey, Canada) installed on a Leica MZ16 stereomicroscope (Leica Microsystems, Wetzlar, Germany) was used to take low magnification optical images (32x). The optical images were analyzed with the aid of QCapture Pro software (QImaging, Surrey, Canada).

Table 1: Building Parameters

Build orientation	Raster angle	Default Parameter			Insight revision method			Visual feedback method		
		CW	RW	RRAG	CW	RW	RRAG	CW	RW	RRAG
XYZ	0°/90°	0.508	0.508	0	0.432	0.432	0	0.432	0.432	-0.013
	30°/-60°	0.508	0.508	0	0.432	0.432	0	0.432	0.432	-0.013
	45°/45°	0.508	0.508	0	0.432	0.432	0	0.432	0.432	-0.013

\*CW= Contour Width, RW= Raster Width, RRAG= Raster to Raster Air gap

\*\* All the values are in mm

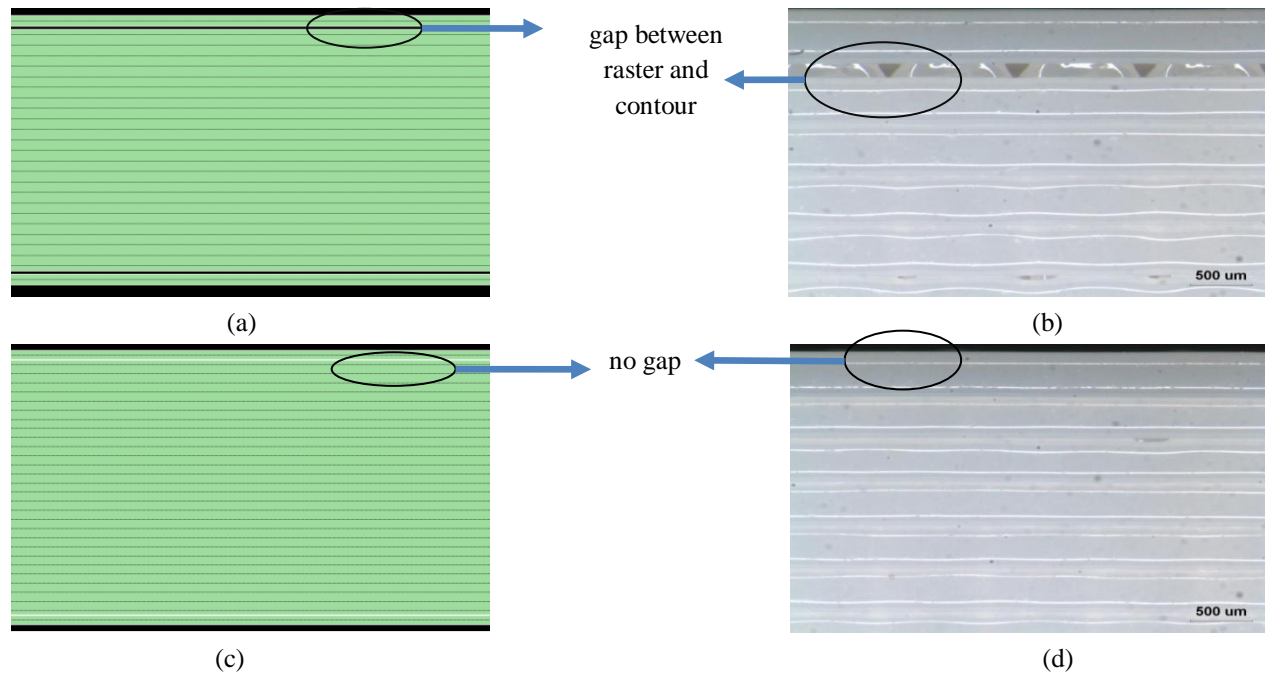
### Mechanical Testing:

Tensile tests were carried out by using an Instron 5866 (Instron, Norwood, MA) tensile testing machine, which had a load cell of 10 kN. The load cell measurement accuracy was  $\pm 0.4\%$  (as per manufacturer's specifications). The ramp speed was kept to a constant 5 mm/min. The UTS, Young's modulus, and tensile strain were calculated by the built-in software, Bluehill (Instron, Norwood, MA). Five specimens (totaling 45) were tested for every parameter modification. Before mechanical testing, all specimens were conditioned for 40 hours at 23 °C and 50% relative humidity, according to ASTM standard D618 [14].

## Results and discussion

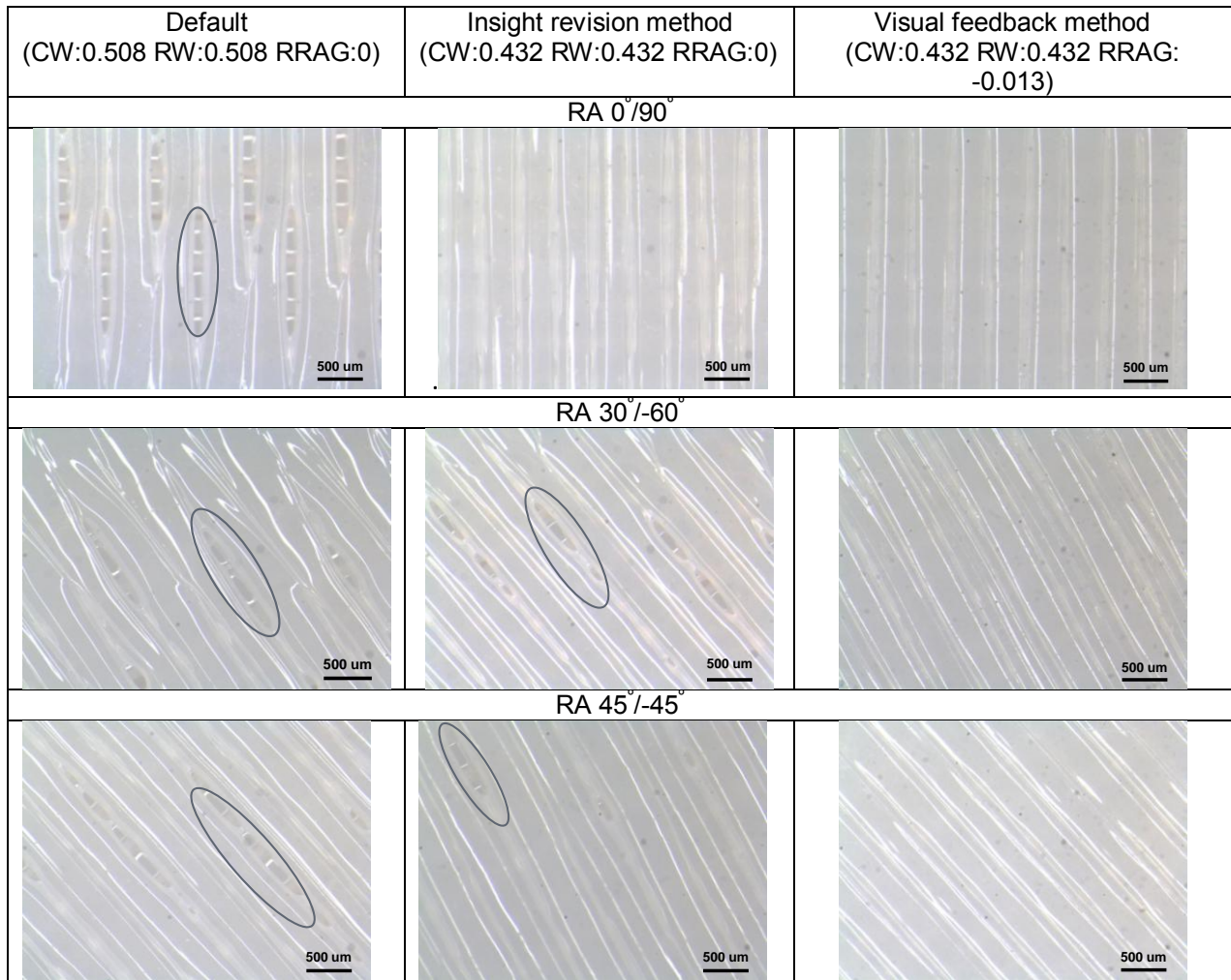
### Optical Observations:

Fig. 4 shows the optical images of rendered toolpaths created by Insight and actual material deposition. In the Fig. 4, using the default parameters, the gaps between contour and rasters are visible (Fig. 4a and 4b). Fig. 4c and 4d show that, using modified parameters (Insight revision method, contour width at 0.432 mm and raster width at 0.432 mm), gaps between the contour and rasters were removed.



**Fig. 4** Rendered toolpaths generated by Insight (left) and actual deposited material (right) for the XYZ orientation using a  $0^\circ/90^\circ$  raster angle; a) and b) default parameters (CW 0.508 mm, RW 0.508 mm, RRAG 0 mm), c) and d) Insight revision method parameters (CW 0.432 mm, RW 0.432 mm, RRAG 0 mm)

Despite the efforts to remove air gaps with Insight revision, some gaps could be seen which were not visible in Insight renderings. Fig. 5 shows more detailed observations of the three methods used: default method, Insight revision method, and visual feedback method. This figure shows the optical imaging observations for the XYZ build orientation using RAs at  $0^\circ/90^\circ$ ,  $30^\circ/60^\circ$ , and  $45^\circ/45^\circ$ . Gaps can be seen between adjacent rasters using default values (CW at 0.508 mm, RW at 0.508 mm, and RRAG at 0 mm). Using Insight revision, CW and RW were decreased, (CW at 0.432 mm, RW at 0.432 mm, and RRAG at 0 mm) and gaps between rasters were reduced. The gaps were completely removed using visual feedback modifications (CW at 0.432 mm, RW at 0.432, and RRAG at -0.013 mm).



**Fig. 5** Optical images of specimens built in the XYZ orientation with air gaps highlighted by black circles (parameters are set in mm)

Mechanical Testing Results

The UTS results obtained for the three RAs are presented in Fig. 6. For all the RAs, the greatest increase in UTS was obtained with the visual feedback method, compared to the UTS obtained using default parameters. The negative RRAG led to a decrease in gaps between rasters, which is the reason for the increase in UTS. This is supported by Ahn *et al.* who indicated negative RRAGs led to stronger, denser, structures [11]. The highest percent increase in UTS compared to the default was 19% (44.76 MPa vs. 53.22 MPa), obtained using a 30°/-60° RA. The percent increases for all three RAs are listed in Table 2.

A two sample t-test showed that UTS results acquired with the default parameters and visual feedback method were significantly different (p value < 0.05). The t-test results are listed in Table 3. The ANOVA test (table 4) shows that UTSS, among different RAs, are not significantly different (p value > 0.05) using same build method. Whenever the RA was changed, the delta angle (change of raster angles between two adjacent layers) was kept constant at 90°. Thus, the directional effect of one layer might be nullified by the delta angle of the adjacent layer. This might be the reason behind the lack of significant differences in UTS when changing RA. However, this statement is not supported by Masood et al. [10] who observed a change in UTS using different RAs. Their observations were not statistically analyzed.

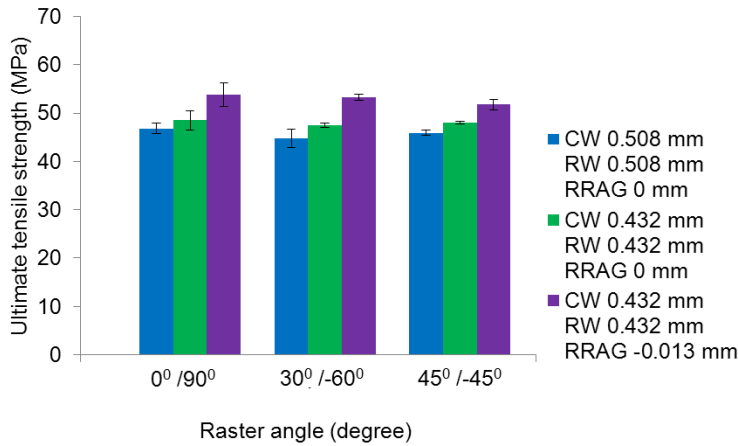


**Fig. 6** UTS for XYZ build orientation using three different RAs. Each bar represents the average of at least 5 specimens and the error bars are +/- standard deviation

Table 2: Percentage of UTS increase relative to UTS from the default method for the XYZ build orientation

Raster angle	Insight revision method	Visual feedback method
0°/90°	4%	15%
30°/-60°	6%	19%
45°/-45°	5%	13%

Table 3: t test results for comparison of UTS with default and visual feedback methods

Build Orientation	Raster angle	Sample 1	Sample 2	t statistical	t critical (two/one tail)	p-value
XYZ	0°/90°	Default	Visual feedback	5.11	2.30	9e-04
	30°/-60°	Default	Visual feedback	8.51	2.57	9e-04
	45°/-45°	Default	Visual feedback	9.65	2.30	1e-05

Table 4: ANOVA table for UTS

Build orientation	Design Parameters	Sample 1	Sample 2	Sample 3	Df <sub>total</sub>	F Value	F Critical	P Value
XYZ	Default	0°/90°	30°/-60°	45°/-45°	14	2.54	3.88	0.120
	Insight revision	0°/90°	30°/-60°	45°/-45°	14	0.70	3.88	0.511
	Visual feedback	0°/90°	30°/-60°	45°/-45°	14	1.64	3.88	0.234

Fig. 7 shows the Young's modulus for XYZ build orientation. The highest average Young's modulus achieved was 1816 MPa. This was obtained using a 0°/90° RA with the visual feedback method (compared to 1595 MPa with the default). Analysis of the optical images, led to the understanding that changes in Young's modulus may be directly related to removal of air gaps. For example, in Fig. 5, for all three RAs, removal of gaps is visible with the visual feedback method, compared to other two methods. Hence, there is an increase in Young's modulus.

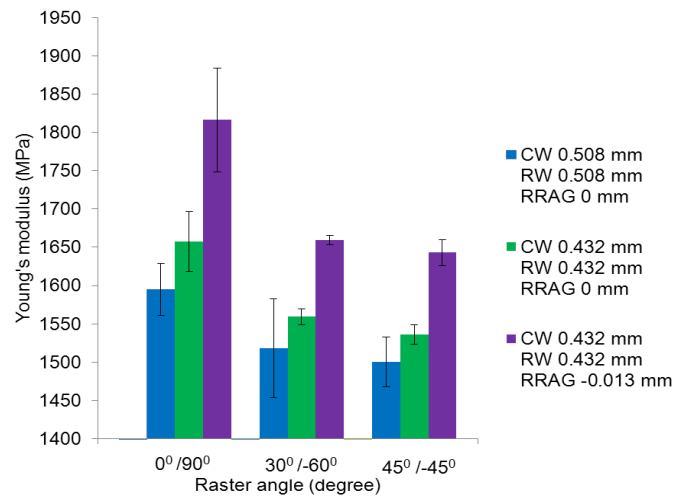
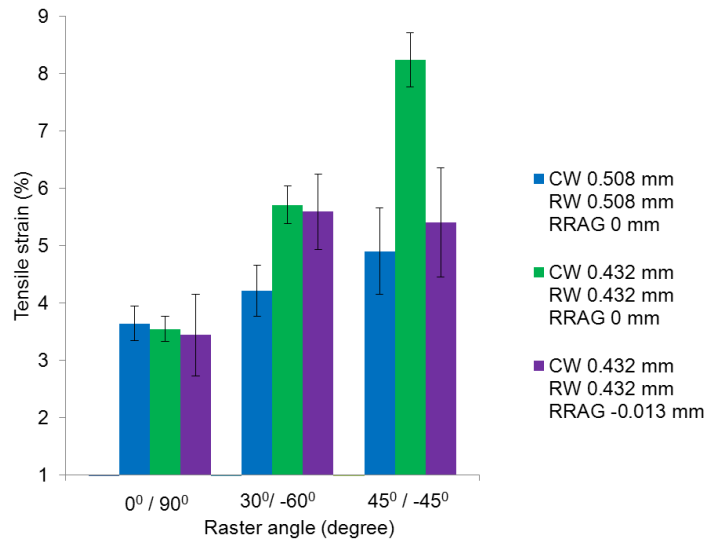


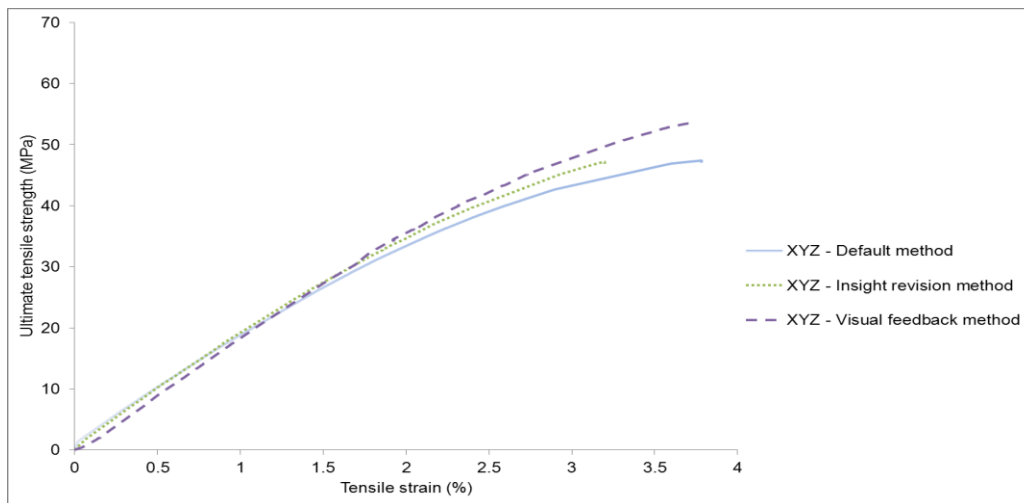
Fig. 7 Young's modulus for XYZ build orientation. Each bar represents the average of at least 5 specimens and the error bars are +/- standard deviation

Fig. 8 represents the tensile strain values for the XYZ build orientation using the three RAs. The highest average tensile strain obtained was just over 8% for the 45°/-45° RA with the Insight revision method. The values typically varied from 3.5% - 8%. Nadooshan et al. reported a maximum tensile strain of 5% using PC [15]. With the modification in build parameters, higher values of tensile stain are achievable.

Fig. 9 shows the characteristic stress-strain curves for the above mentioned results. It illustrates the curves closest to the average values obtained for the 0°/90° RA using the default, Insight revision, and visual feedback methods. The figure only illustrates the 0°/90° RA as there was no significant difference in UTS amongst different RAs. This graph helps to get an understanding of the benefits achievable from performing the methods discussed in this paper.



**Fig. 8** Tensile strain for XYZ build orientation. Each bar represents the average of at least 5 specimens and the error bars are +/- standard deviation



**Fig. 9** Characteristic stress-strain curves for three methods using 0°/90° RA. Default method is represented by a solid line (blue), Insight revision method by a round dotted line (green), and visual feedback method by a dashed line (purple).

## **Conclusion**

Building parameters (including RA, RW, CW, and RRAG) play a vital role in improving mechanical properties of FDM-produced parts. In all circumstances, parameter modification using the Insight revision method, improved UTS compared to default values. The visual feedback method further improved UTS, introducing negative RRAGs, which led to an average increase in UTS of 16 % compared to the specimens built with default parameters. Overall, the highest average value of UTS obtained for PC was 53.75 Mpa (compared to 46.84 MPa with the default). Optical imaging, or the visual feedback method, provided great assistance in improving mechanical properties. Optical observations also led to the realization that what was rendered by the insight job file, was not necessarily what was produced. Air gaps were present in the final specimens, despite that those gaps were not visible in the job file created by Insight. Therefore, a separate calibration protocol or an in-situ monitoring system can identify necessary adjustments to the processing parameters. Introducing negative RRAGs created stronger inter-raster bonding and minimized or even removed gaps (at least through optical imaging observations) between rasters. Future work may include the effect of build orientation as well as layer thickness in further improving mechanical properties of FDM parts. However, modifications in layer thickness may compromise building time. While the visual feedback method does reduce the gaps in a part, it does not completely eliminate them. Therefore, measurements can be conducted in the future to determine how the changes in porosity of the samples, through the elimination of air gaps, affect density.

## **Acknowledgement**

The research presented here was conducted at The University of Texas at El Paso (UTEP) within the W.M. Keck Center for 3D Innovation (Keck Center), recently expanded to over 13,000 sq. ft. The W.M. Keck Center provides access to state-of-the-art facilities and equipment as a result of funding from the State of Texas Emerging Technology Fund. Financial support for the research was provided, in part, by the University of Texas System Louis Stokes Alliance for Minority Participation Program under grant NSF-HRD-1139929 as well as the Mr. and Mrs. MacIntosh Murchison Chair I in Engineering Endowment. The authors would like to acknowledge Mr. Luis A. Ochoa for his assistance in various aspects of this research.

## References

- [1] "(2012) Standard Terminology for Additive Manufacturing Technologies. ASTM International. Designation: F2792-12a".
- [2] "Stucker B (2012) Additive manufacturing technologies: technology introduction and business implications. In: *Frontiers of engineering; reports on leading-edge engineering from the 2011 symposium*. National Academies Press, Washington DC, pp 5-14".
- [3] Q. Sun, G.M. Rizvi, C.T. Bellehumeur, P. Gu, (2008), "Effect of processing conditions on the bonding quality of FDM polymer filaments" *Rapid Prototyping Journal*, Vol.14 Iss:2 pp. 72-80.
- [4] "Swanson WJ, Turley PW, Leavitt PJ, Karwoski PJ, LaBossiere E, Skubic RL (2004) High Temperature Modeling Apparatus. United States Patent. US 6,722,872 B1".
- [5] "Perez M, Block M, Espalin D, Winker R, Hoppe T, Medina F, Wicker R (2012) Sterilization of FDM-manufactured parts. In: *Proceedings of the 2012 Annual International Solid Freeform Fabrication Symposium*, Austin, TX, USA."
- [6] Zein I, Dietmar WH, Tan KC, Teoh SH (2002) Fused deposition modeling of novel scaffold architectures for tissue engineering applications. *Biomaterials* 23:1169-1185.
- [7] Espalin D, Arcaute K, Rodriguez D, Medina F, Posner M, Wicker R (2010) Fused deposition modeling of patient-specific polymethylmethacrylate implants. *Rapid Prototyping J* 16:164-173. doi: 10.1108/13552541011034825.
- [8] Kalita SJ, Bose S, Hosick HL, Bandyopadhyay A (2003) Development of controlled porosity polymer-ceramic composite scaffolds via fused deposition modeling. *Mater Sci Eng* 26:611-620.
- [9] Masood SH, Song WQ (2004) Development of new metal/polymer materials for rapid tooling using fused deposition modeling. *Mater Design* 25:587-594.
- [10] "Masood SH, Mau K, Song WQ (2010) Tensile properties of processed FDM polycarbonate material. *Mater Sci Forum* 654-656:2556-2559. doi: 10.4028/www.scientific.net/MSF.654-656.2556".
- [11] "Ahn SH, Montero M, Odell D, Roundy S, Wright PK (2002) Anisotropic material properties of fused deposition modeling ABS. *Rapid Prototyping J* 8:248-257. doi:

10.1108/13552540210441166".

- [12] "Sood AK, Ohdar RK, Mahapatra SS (2010) Parametric appraisal of mechanical property of fused deposition modelling processed parts. Mater Design 31:287-295".
- [13] "(2010) Standard Test Method for Tensile Properties of plastics. ASTM International. Designation: D638-10".
- [14] "(2008) Standard Practice for Conditioning Plastics for Testing. ASTM International. Designation: D618-08".
- [15] "Nadooshan AA, Daneshmand S, Aghanajafi C (2007) Application of RP technology with polycarbonate material for wind tunnel model fabrication. Proc Wrlld Acad Sci E 26."